

# *In situ* microscopic structural investigations with a three-dimensional X-ray microscope: nano3DX

Kazuhiko Omote\*, Yoshihiro Takeda\*, Raita Hirose\* and Joseph D. Ferrara\*\*

## 1. Introduction

It is well known that X-rays can penetrate opaque objects and show the internal structure without destroying the object. Thus, X-rays are widely used for medical imaging, security and industrial inspection to name a few examples. In addition, X-ray computed tomography (CT) is a powerful technique for visualizing internal structure of various specimens including the human body, in three dimensions (3D). Recently, a high spatial resolution X-ray microscope has been developed as a result of improvements in microfocus X-ray sources and high resolution X-ray detectors, making it possible to determine the precise internal 3D structure at micrometer resolution. Rigaku has developed a unique 3D X-ray microscope, the nano3DX, by the application of the quasi-parallel beam technique with a rotating anode high-power X-ray source and submicron-resolution X-ray detector<sup>(1)</sup>. An additional feature of the nano3DX is that it provides the ability to obtain high-contrast CT images for low-Z materials utilizing relatively low energy X-rays, e.g., Cu or Mo characteristic radiation. This feature of the nano3DX makes it very well suited for structural studies and/or inspection of various low-Z materials, e.g., polymer composite, pharmaceutical tablets, biomaterials and foods. Conventional X-ray microscopes use high energy tungsten white radiation to probe the specimen. The high energy X-rays make it difficult to distinguish constituent low-Z components from each other due to their low absorption. In addition, there is also demand for precise investigation of structural changes induced by changes in environmental conditions, for example, temperature variations or application of compression or tensile stress. In order to investigate structural changes under real environmental conditions, it was necessary to build *in situ* attachments, which can be combined with CT measurements.

In conventional CT systems (fan or cone beam), it is necessary to take a large number of projection images while rotating sample 360 degrees. However, with the quasi-parallel beam of the nano3DX, only 180 degrees of data are needed due to the inversion symmetry of the projection data. In order to realize the acquisition of projection images within 180 degrees rotation without any blind region, 1) the cell should be covered by X-ray transmissive materials, e.g., plastics,

or 2) should provide for non-contact heating or cooling as the sample rotates. In this paper, we will first describe the construction of the *in situ* attachments. Next, we will present experiments displaying dynamic changes in three-dimensional structures induced by changing temperature and applying pressure.

## 2. Description of *in situ* examination devices

### 2.1. Elevated temperature and compression attachment

Figure 1 shows photograph of the nano3DX attached with the high temperature/compression attachment. The top part is a pressure actuator with motor. A pressure probe is placed between the actuator and the pressure-transmission piston. A heater and a thermocouple are also incorporated into the device. Therefore, compression and elevated temperature can be applied simultaneously. The maximum temperature and pressure are restricted by the material of outer shell, which should be made from a material which minimally absorbs X-rays. In the present implementation the window is made from a heat-resistant plastic that allows



**Fig. 1.** Photograph of the elevated temperature and compression attachment. The pressure is applied by the actuator with the drive motor located above the sample. The outer shell is made from a heat-resistant plastic that allows for temperature up to 200°C and force up to 200 N.

\* X-ray Research Laboratory, Rigaku Corporation.

\*\* Rigaku Americas Corporation.

for temperature up to 200°C and force up to 200 N. As shown in Fig. 1, there are no additional supports around the shell and no blind region for the acquisition of complete projection data for CT reconstruction. In addition, the X-ray window area is made thinner in order to increase the transmitted X-ray intensity. In the section 3.1, we will show microscopic structural changes in shock absorbing resin foam by applying compression.

**2.2. Variable temperature attachment**

This device can provide a temperature range of from -20°C to +100°C using a Peltier element as shown in Fig. 2. The attachment consists of a thermally conductive metal stage covered by a transparent plastic shell. The lower part includes heat dissipating fins which are cooled by airflow from a fan. One of interesting applications of this device is to measure the behavior of gels or emulsions. It is difficult to acquire complete projection data for CT reconstruction on these samples due to fluidity. We can expect the movement in such



**Fig. 2.** Photograph of the variable temperature attachment, which allow a temperature range of from -20°C to +100°C. A sample is placed in a transparent plastic shell.

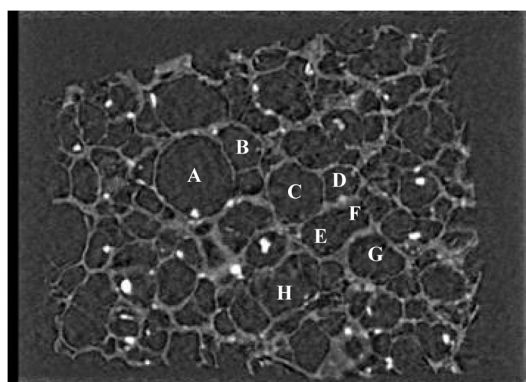


**Fig. 3.** Photograph of the non-contact high-temperature attachment, which is suspended by the side arm and covers the sample without contacting it. X-rays are transmitted through the fixed incident and exit windows.

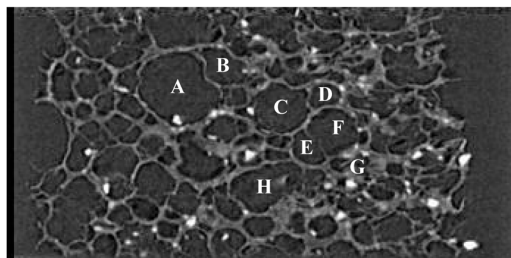
a sample to be reduced at lower temperature, making measurements possible. With this attachment, it is also possible to investigate the behavior of oils and their mixtures with melting points around room temperature. Here, we will show the three-dimensional structure for a water-oil mixture at the freezing point in section 3.2.

**2.3. Non-contact high-temperature attachment**

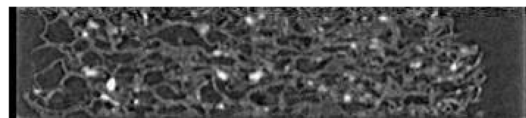
In order to investigate time dependence of the changes in internal structure caused by changes in environmental conditions, such as temperature, it is useful to collect CT data continuously (so called four dimensional (4D) CT). For such purpose, it is



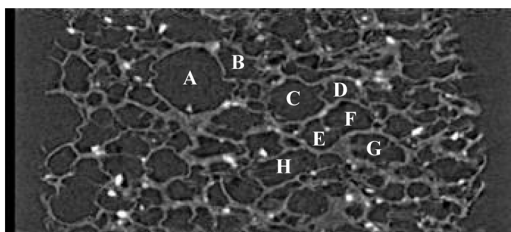
(a) 0 MPa



(b) 7 MPa



(c) 14 MPa



(d) 0 MPa

**Fig. 4.** Tomographic images for (a) no pressure 0Pa, (b) 7MPa, (c) 14MPa, and (d) release pressure of 0Pa, respectively, using the elevated temperature and compression attachment. In order to make identification of individual pores easier, eight representative pores have been labeled A to H.

preferable to rotate the sample continuously during data acquisition. However, because *in situ* attachments usually have cables for heaters and thermocouples, it is difficult to rotate the attachment more than one revolution. Therefore, we have developed a heating device, which does not have direct contact with sample and its rotation stage. As shown in Fig. 3, the heating device is suspended by the side arm and rotates the sample from the top. The incident and exit window positions are fixed and X-rays always pass through these windows. We have confirmed it is possible to raise temperature to more than 200°C at the sample position with this device. We will show an example of the change of internal structure as the temperature raised in section 3.3.

### 3. Examples of *in situ* measurements

#### 3.1. Structural change by compression

The measurement sample is a section of a cushion from the sole of a shoe. This cushion was cut into a small piece of cubic shape about 0.6 mm on a side and placed between the two pistons of the pressure/temperature attachment device shown in Fig. 1. The resultant tomographic images are shown in Fig. 4 for (a) no pressure 0 Pa, (b) 7 MPa, (c) 14 MPa, and (d) release pressure of 0 Pa, respectively. It is easy to recognize that the sample is made of foam rubber from the images, with a typical wall thickness of a few micrometers. When pressure is applied, each pore becomes deformed and crushed. We placed labels, A to H, on representative pores to make it easy to recognize those individual pores. At 7 MPa, every pore is deformed and crushed in the vertical direction, but almost all of the pores still remain. We can also see that deformation of upper area, in contact with the piston, is larger than that of center area. At 14 MPa, it seems almost all pores are completely crushed. This pressure is much higher than would be seen in normal use of the shoe. However, when the pressure is released, we observe the pores, A through H, do not fully recover to their original size. In order to investigate deformation of the pores more

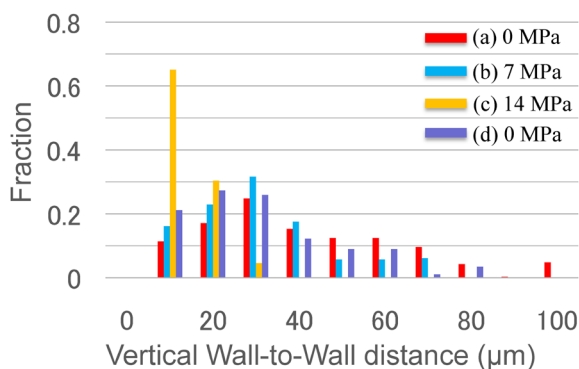


**Fig. 5.** Fractional distribution of the vertical distances (top wall to bottom wall) of the pores shown in Fig. 4. The distances decrease with increasing pressure.

precisely, we have measured the distances from the top to the bottom walls of the pores and calculated their distribution functions as shown in Fig. 5. As you can see the number of larger inter-wall distances are decreasing while the number of smaller inter-wall distances are increasing with application of pressure. This attachment can also raise the sample temperature up to 200°C allowing the investigation of structural changes with both variable temperature and pressure.

#### 3.2. CT measurement of a water and oil mixture

Gel materials such as cosmetics and toothpastes are complex mixtures of a number of functional materials and are fluid at the room temperature. CT imaging could be useful to investigate the dispersion states of those materials in three dimensions. By using the low temperature attachment introduced in 2.2, we can fix motion such materials and allow the acquisition of projection data for CT reconstruction. This particular sample is a mixture of water and edible oil, which is liquid at room temperature. The CT image for this

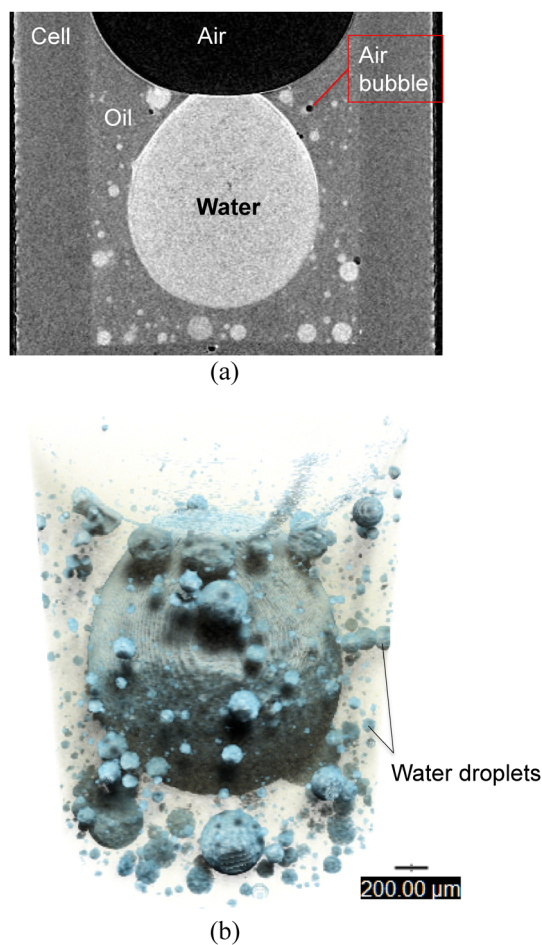


**Fig. 6.** (a) Tomographic images for the frozen oil-water mixture, white bubbles are water droplets and the grey area is oil, (b) Three-dimensional rendering of the mixture.

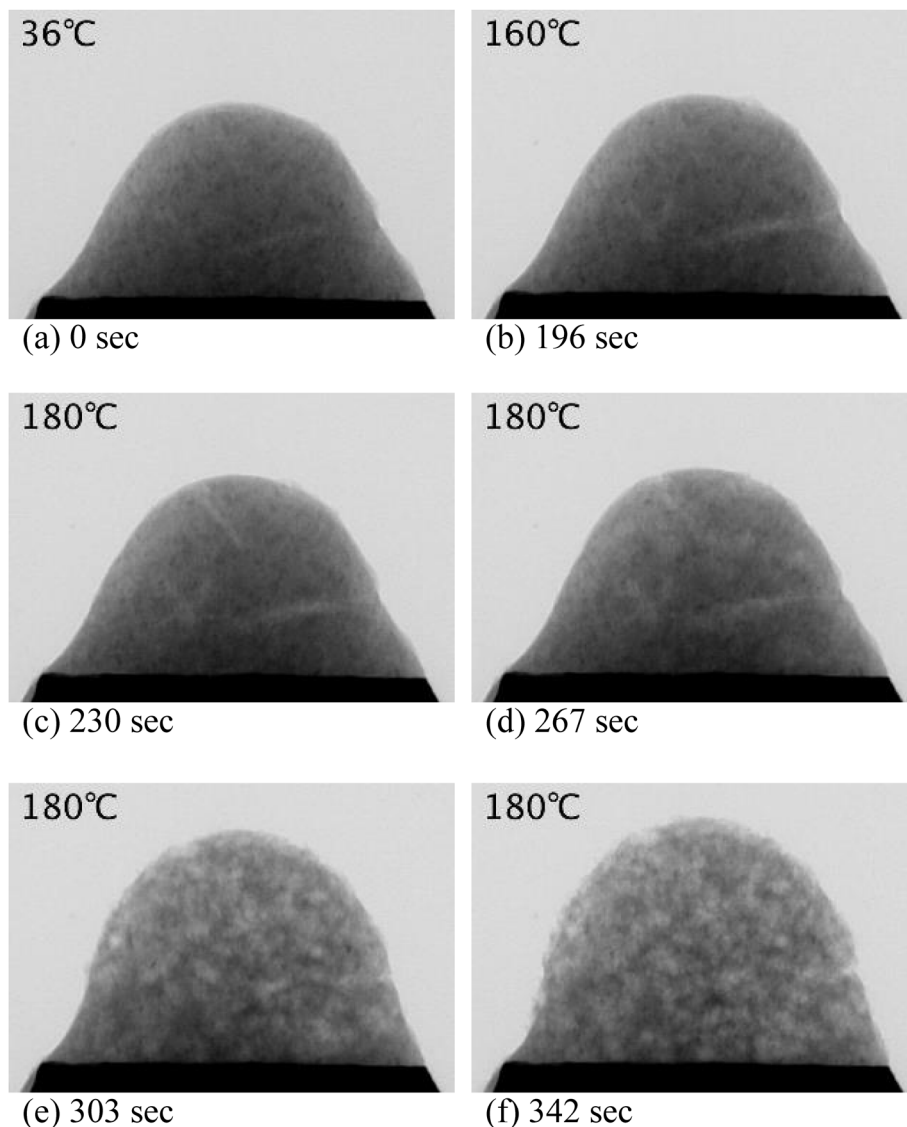


**Fig. 7.** Projection images of heat forming polymer with raising temperature. The volume continues to grow even though temperature has been kept at 180°C.

material in the frozen state of this mixture at  $-20^{\circ}\text{C}$  is shown in Fig. 6(a). The large, white colored droplet visible in the center area is water. There are also many small water droplets that can be seen around it, with some droplets having a diameter less than  $10\mu\text{m}$ . One can also observe small black features, which are air bubbles confined in the mixture. Figure 6(b) is three-dimensional visualization of the same sample and we can clearly recognize how water droplets are dispersed in the mixture.

### 3.3. Continuous CT measurements over an extended time period

Heat-initiated polymer foam capsules display a very large volume expansion as the temperature is raised. The generated foam is light and soft, and is used as filler and shock absorbent material, for example. In order to investigate the foaming process as a function of

temperature, we have examined continuous acquisition of projection data during as the temperature is raised from  $36^{\circ}\text{C}$  to  $180^{\circ}\text{C}$  at a rate of  $35\text{K}/\text{min}$ . Several typical images are shown in Fig. 7. The exposure time per image is 2 sec. One can see the volume of the sample continues to increase even at the final temperature of  $180^{\circ}\text{C}$ . We have measured CTs at both the starting temperature  $36^{\circ}\text{C}$  and final temperature  $180^{\circ}\text{C}$  and results are shown in Fig. 8. One can see a lot of voids are created in the sample at  $180^{\circ}\text{C}$ , caused by the foaming of the polymer. To qualitatively understand the distribution of voids, we measured the volume of the voids and display a three-dimensional color mapping of the void volumes, shown in Figs. 9(a) and 9(b). In addition, the void diameter distribution is shown in Fig. 9(c). The voids from  $50\mu\text{m}$  to  $80\mu\text{m}$  in diameter are the major components of the distribution, but there are also many voids that have more than  $100\mu\text{m}$  in diameter.

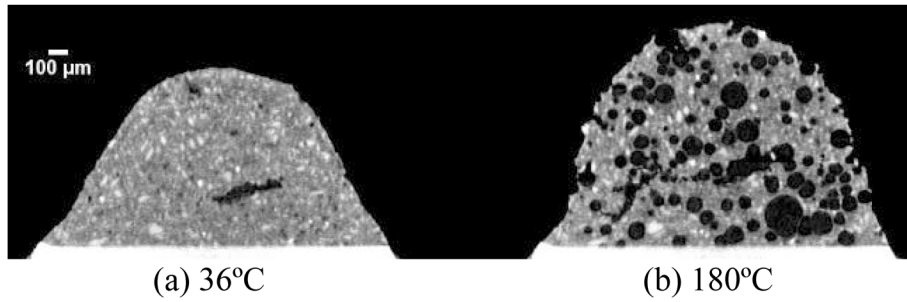
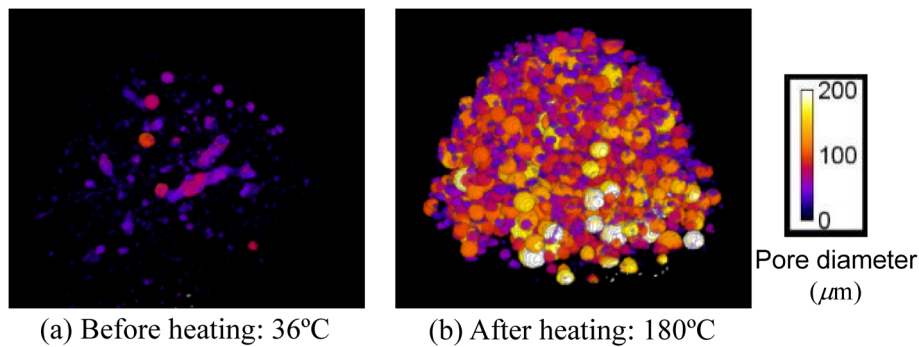
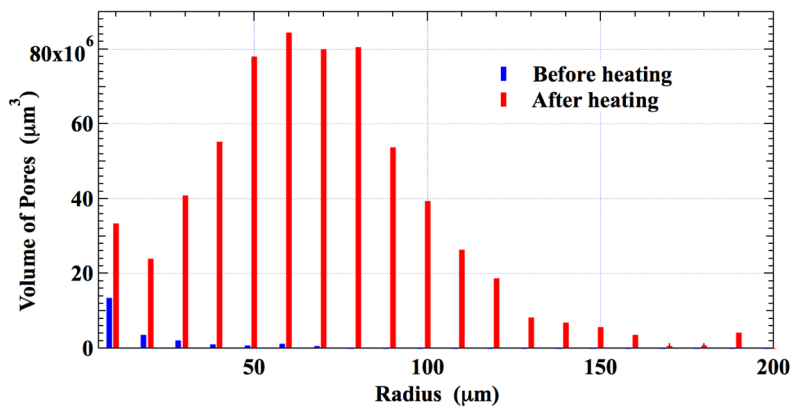


Fig. 8. Tomographic images (a) before and (b) after expansion. Note the number of pores that form in the expanded sample.



(a) Before heating: 36°C (b) After heating: 180°C



(c) Pore size distribution

Fig. 9. 3D renderings of the pores (a) before and (b) after expansion. White on the color scale indicates larger diameter pores, (c) volume distribution of pore radius.

A continuous 4D CT experiment was also tried to obtain in order to investigate structural evolution with expanding-foam capsules. The resultant three-dimensional images are shown in Fig. 10. The measurement time of every CT image is 9sec and each CT image interval is 36sec and pixel size of the images are  $5.2\mu\text{m}$ . Thus, it took 180sec from Figs. 10(a) to 10(f) and with the temperature changing from  $140^\circ\text{C}$  to  $180^\circ\text{C}$ . The resolution of each 3D image is not the maximum of the instrument because of the short exposure times, but we can obtain dynamic evolution of

internal structure in the sample by means of 4D CT.

#### 4. Conclusion

We have developed three *in situ* attachments for the nano3DX which enable the experiments at variable temperature and pressure. We demonstrate three examples: 1) distortion of the pores in a foam rubber cushion from a shoe, 2) dispersion in a water-oil mixture, and 3) thermal expansion of a micro-foaming capsule. By using these *in situ* attachments, it is possible to investigate precise the three-dimensional structural

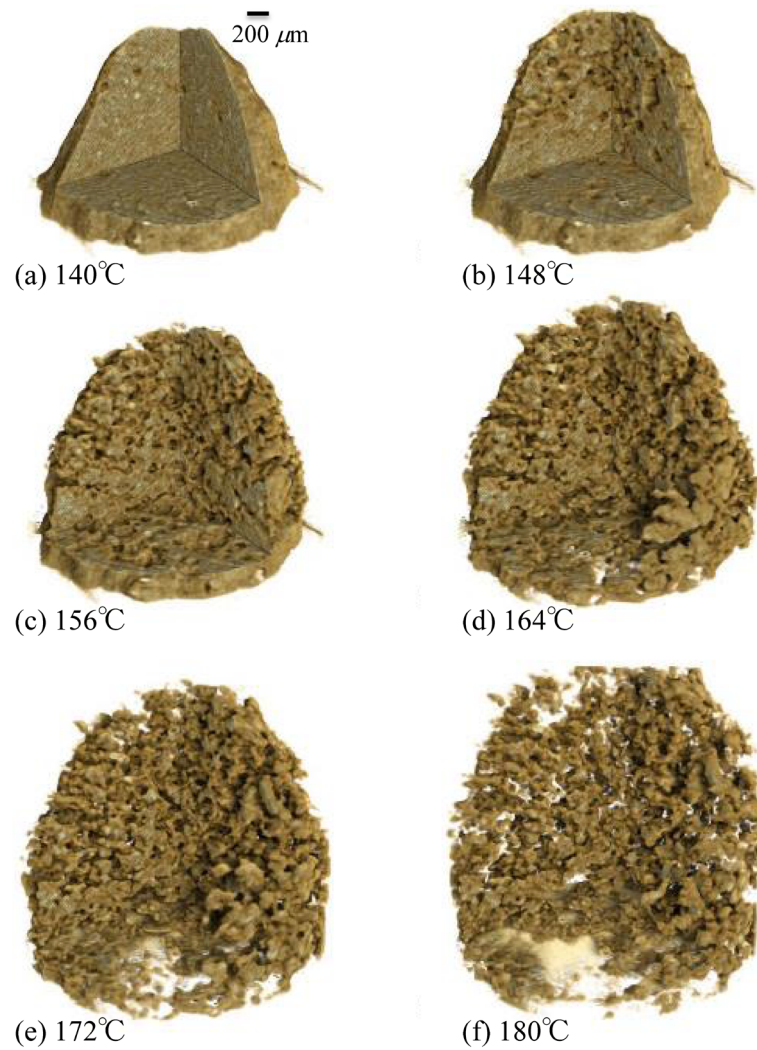


**Fig. 10.** 3D renderings visualizing the expansion of a heat-initiated polymer foam from (a) 140°C to (f) 180°C. Note that the number of pores increases as does the volume of each pore as the temperature rises. This time-dependent data were collected by continuous 4D CT measurement.

change of functional materials in microscopic scale. *In situ* attachments, we have introduced in this paper, could be very useful to study and understand characteristics of functional materials under real conditions.

#### Reference

- (1) Y. Takeda and K. Hamada: *Rigaku Journal (English version)*, **30** (2014), No.1, 17–22.